Inorganic Chemistry

Article

pubs.acs.org/IC

Cobalt in a Bis-β-diketiminate Environment

Michael P. Marshak, Matthew B. Chambers, and Daniel G. Nocera*

Department of Chemistry, 6-335, Massachusetts Institute of Technology, 77 Massachusetts Avenue, Cambridge, Massachusetts 02139-4307, United States

Supporting Information

ABSTRACT: The reaction of $Co_2(mesityl)_4$ with acetonitrile leads to the formation of a planar, low spin, bis-β-diketiminate cobalt(II) complex, $(1\text{-mesitylbutane-1,3-diimine})_2Co$ (**1**). EPR spectroscopy, magnetic studies, and DFT calculations reveal the Co(II) ion to reside in a tetragonal ligand field with a $^2B_2(d_{yz})^1$ ground state electronic configuration. Oxidation of **1** with ferrocenium hexafluorophosphate furnishes $(1\text{-mesitylbutane-1,3-diimine})_2Co(THF)_2PF_6$ (**2**). The absence of significant changes in the metal−ligand bond metrics of the X-ray crystal structures of **1** and **2** supports ligand participation in the oxidation event. Moreover, no significant changes in C−C or C−N bond lengths are observed by X-ray crystallography upon oxidation of a β-diketiminate ligand, in contrast to typical redox noninnocent ligand platforms.

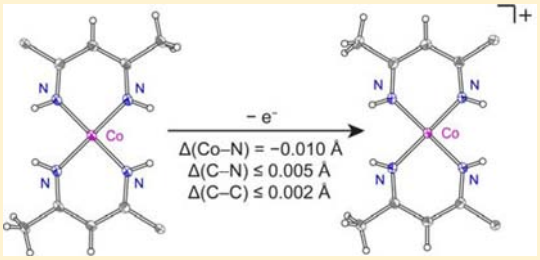

INTRODUCTION

The oxidation or reduction of a metal often causes significant structural changes to reflect the differing electronic structure of the system. Catalytic processes that involve a change in oxidation state thus confront energy barriers to reorganization. The use of ligands that can participate in redox chemistry is one method to facilitate multielectron redox processes and minimize the inherent geometric and electronic energy barriers that transition metals may incur. Although organic ligands are not immune to structural changes upon oxidation or reduction, the resulting organic radicals are usually delocalized over the ligand, minimizing reorganizational energy. In pursuit of attaining facile multielectron redox chemistry, our group has investigated porphyrin,[1−3] corrole,[4−6] porphyrinogen,[7−10] and PNP pincer[11] complexes containing redox noninnocent ligand systems. These properties have been exploited to facilitate the two- and four-electron processes involving hydrogen and oxygen, respectively.[12,13]

One common motif in many of these redox noninnocent ligands is the presence of energetically accessible π bonding molecular orbitals.[14] The delocalization that occurs in π bonding yields a small gap in the HOMO−LUMO levels, placing one of these levels proximate or within the d-orbital manifold of the metal. Accordingly, electrons can be gained by or removed from ligand based orbitals rather than metal d-orbitals upon oxidation or reduction of the metal complex.

Most π-based redox-active ligands studied to date contain an even number of atoms in the framework to generate an equal number of π bonding and antibonding orbitals.[15−19] By changing the electronic occupancy of these orbitals, the ligand bond distances are expected to change. For example, bipyridine can coordinate to transition metals in its neutral, monoanionic, or dianionic form.[20] Detailed X-ray structural analysis has shown that the reduction of bipyridine corresponds to a successive increase in the C1−C1′ bond length by roughly 0.05 Å for each electron added.

Conversely, β-diketiminate (NacNac) ligands have an odd number of atoms in its backbone. Despite their ubiquitous presence in transition metal chemistry,[21,22] only recently have Khusniyarov and Wieghardt shown NacNac ligands to be redox-active.[23] Pseudotetrahedral nickel bis-NacNac forms an intensely colored complex upon its oxidation at −20 °C. This oxidized complex has been described as a Ni(II) NacNac radical cation rather than a Ni(III) complex, based on DFT calculations and strong visible absorptions. Owing to the odd number of orbitals in the π system, the HOMO of a NacNac ligand is a π nonbonding orbital. Corresponding oxidation of this orbital implies that no ligand bond length changes should be detectable by X-ray crystallography leading to the moniker of "hidden noninnocence" to describe a class of ligands that undergo redox events without accompanying observable structural changes.

Herein we describe and characterize a planar $Co(NacNac)_2$ (**1**) system that is synthesized by the activation of acetonitrile. The convenient synthesis of NacNac from organometallic precursors and acetonitrile provides a new route to generate late transition metal N−H functionalized NacNac complexes. Oxidation of **1** yields the first crystallographically characterized NacNac based radical in a metal complex. The nature of this ligand-based cation radical is compared to those derived from other macrocyclic ligands.

EXPERIMENTAL SECTION

General Considerations. All reactions were performed in a nitrogen filled glovebox or by using standard air-free Schlenk

Received: September 9, 2012
Published: September 26, 2012

   dx.doi.org/10.1021/ic301970w | *Inorg. Chem.* 2012, 51, 11190−11197

techniques. Solvents were dried by passage through a column of activated alumina and stored over 4 Å molecular sieves. $Li(THF)_4CoMes_3$,[24] $[CoMes_2]_2$,[24] and Cp_2FeBAr^F [25] were prepared according to literature procedures. Cp_2FePF_6 was purchased from Sigma-Aldrich. IR spectra of powdered samples were recorded on a PerkinElmer Spectrum 400 FT-IR/FT-NIR spectrometer outfitted with a Pike Technologies GladiATR attenuated total reflectance accessory with a monolithic diamond crystal stage and pressure clamp. NMR and EPR spectra were recorded at the MIT Department of Chemistry Instrumentation Facility on a Varian Mercury 300 NMR spectrometer and a Bruker EMX EPR spectrometer (X band, 9.860 GHz). Magnetic data were collected on benzene solutions of **1** and **2** at room temperature utilizing Evans' method.[26] Magnetic susceptibility data were corrected for diamagnetic contributions for the core diamagnetism of each sample (estimated using Pascal's constants). Elemental analyses were performed by Midwest Microlab LLC.

$Li(THF)_4CoMes_3$ (100 mg, 0.14 mmol) was dissolved in 5 mL of THF, which was cooled to −40 °C. A 5 mL portion of acetonitrile was added dropwise. After standing for 12 h, the solution was warmed to room temperature and then heated to 70 °C for 12 h. The reaction was cooled, and the solvent was removed under vacuum. A dark brown semicrystalline solid was extracted with 3 × 5 mL of diethyl ether, and the solution was filtered, reduced in volume to 2 mL, and placed in a freezer at −40 °C. Two crops of crystals were collected to give 57 mg of **1** as an orange-yellow crystalline solid (88%). ^{1}H NMR (300 MHz, C_6D_6): δ = 4.64 (s, 2H), 1.83 (s, 3H), 0.09 (br s, 6H), −37 (br s, 3H). μ_{eff} = 2.42(5) BM (Evans' method, C_6D_6, 20 °C). UV−vis (pentane): λ_{max}, nm (ε, M^{-1} cm^{-1}) 264 (17 000), 298 (20 600), 377 (12 700), 417 (3600). IR (paratone-*n*, N−H, cm^{-1}): 3297, 3273. Anal. Calcd (Found) for $C_{26}H_{34}N_4Co$: C, 67.7 (67.7); H, 7.4 (7.5); N, 12.1 (12.1). Alternatively, **1** was prepared using $[CoMes_2]_2$ (50 mg, 0.084 mmol), to furnish 27 mg of **1** (70%).

The one-electron oxidized complex, **2**, was prepared from **1**. A 25 mg (0.054 mmol) portion of **1** was dissolved in 3 mL of diethyl ether. Solid Cp_2FePF_6 (18 mg, 0.054 mmol) was added, and the resulting green solution was stirred for 2 h. The solution was filtered, and hexane was added to precipitate dark blue crystals of **2**. The crystals were washed with ether and dried under vacuum to yield 37 mg of **2** (91%). ^{1}H NMR (300 MHz, C_6D_6): δ = 6.42 (s, 3H), 5.79 (s, 3H), 5.19 (s, 3H), 1.32 (s, 1H), 0.42 (s, 1H), −77.44 (br s, 3H). μ_{eff} = 3.2(1) BM (Evans' method, C_6D_6, 20 °C). UV−vis−NIR (THF): λ_{max}, nm (ε, M^{-1} cm^{-1}) 740 nm, 1264 nm. IR (paratone-*n*, N−H, cm^{-1}): 3330, 3266. Anal. Calcd (Found) for $C_{34}H_{50}N_4O_2F_6PCo$: C, 54.4 (54.6); H, 6.7 (6.6); N, 7.5 (7.5).

Electrochemical Details. Cyclic voltammetry experiments were performed in a nitrogen filled glovebox using dry solvents containing 0.1 M Bu_4NPF_6 as a supporting electrolyte. A three compartment cell was employed possessing a glassy carbon electrode as the working electrode, Pt wire as the auxiliary electrode, and Ag/AgCl as a reference electrode. CVs were monitored with scan rates of 10−100 mV/s employing *iR* compensation, and referenced to Cp_2Fe/Cp_2Fe^+.

X-ray Crystallographic Details. Single crystals of **1** and **1a** were obtained by cooling a concentrated solution of ether and acetonitrile, respectively, to −40 °C. Single crystals of **2** were obtained by vapor diffusion of hexane into a concentrated THF solution at room temperature. The crystals were mounted on a Bruker three circle goniometer platform equipped with an APEX detector. A graphite monochromator was employed for wavelength selection of the Mo Kα radiation (λ = 0.710 73 Å). The data were processed and refined using the program SAINT supplied by Siemens Industrial Automation. Structures were solved by direct methods in SHELXS and refined by standard difference Fourier techniques in the SHELXTL program suite (6.10 v., Sheldrick G. M., and Siemens Industrial Automation, 2000). Hydrogen atoms were placed in calculated positions using the standard riding model and refined isotropically. In each case, hydrogens bound to nitrogen were clearly visible in the difference map and refined freely. Refinement of **1** yielded two crystallographically independent molecules, although they were nearly identical to each other. In **2**, the four carbon atoms of the THF molecule that is involved in hydrogen bonding are disordered, and they are modeled using the part command. The minor partition (26%) is restrained with simu and delu commands. The PF_6 ion is also disordered, and the minor partition (7%) is modeled isotropically. Unit cell parameters, morphology, and solution statistics for the structures of **1**, **1a**, and **2** are summarized in Table S1.

Calculations. Density functional theory (DFT) calculations were performed with the hybrid functional Becke-3 parameter exchange functional[27−29] and the Lee−Yang−Parr nonlocal correlation functional (B3LYP)[30] as implemented in the Gaussian 03, Revision B.05 software package.[31] The triple-ζ basis sets with one-set of polarization functions (TZVP)[32] were used for cobalt, nitrogen, and oxygen atoms, and the double-ζ basis sets with one-set of polarization functions (SVP)[33] were used on the carbon and hydrogen atoms. The calculations were performed on truncated models of **1** and **2** where the mesityl groups were replaced with methyl groups. Hydrogen bonding was excluded in all computed models as it was seen to negligibly affect the experimental bonding metrics of **1** versus **1a**. All geometries were confirmed as local minima structures by calculating the Hessians and checking that no negative eigenvalues were present. TD-DFT calculations were performed to calculate the first 50 excited states of each model. Cartesian coordinates of the optimized geometries and absolute energies are provided in the Supporting Information (SI).

RESULTS

Activation of Acetonitrile to NacNac. Treatment of either $Li(THF)_4CoMes_3$ or $[Co(Mes)_2]_2$ with excess acetonitrile yields a brown crystalline solid of (1-mesitylbutane-1,3-diimine)$_2$Co (**1**).

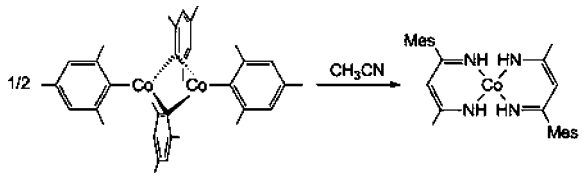

(1)

While this reaction proceeds slowly at or below room temperature, the reaction rate can be accelerated by mild heating. The ^{1}H NMR spectrum indicates the formation of a paramagnetic complex and shows four broad features, which have been assigned as mesityl and methyl groups accordingly (Figure S1). There is no evidence for the α-C−H or N−H resonances of the ligand owing to the delocalization of the SOMO on these atoms (vide infra).

Reaction with CD_3CN shows deuterium incorporation at the in-plane methyl group, and the IR reveals N−D stretching absorptions (Figure S3). The pattern of deuterium incorporation suggests that **1** is formed by insertion of acetonitrile into the cobalt−mesityl bond, followed by attack on a second coordinated acetonitrile (Scheme 1). This mechanism of acetonitrile insertion has been proposed in a scandium−

Scheme 1

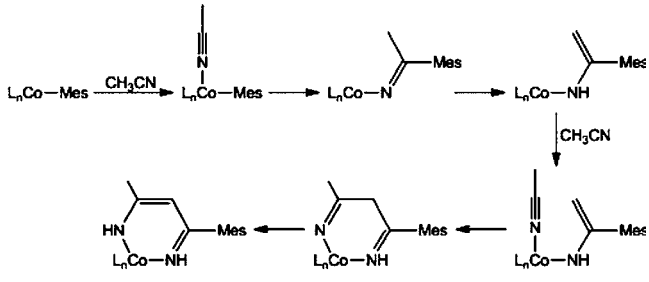

dx.doi.org/10.1021/ic301970w | Inorg. Chem. 2012, 51, 11190−11197

methyl,[34] yttrium−aryl,[35] and chromium−methyl species,[36,37] each of which form corresponding NacNac derivatives.

Characterization of 1. X-ray crystal structures of **1** have been obtained from crystals grown from solutions of both acetonitrile (**1a**) and ether (**1**). As illustrated in Figure 1, both

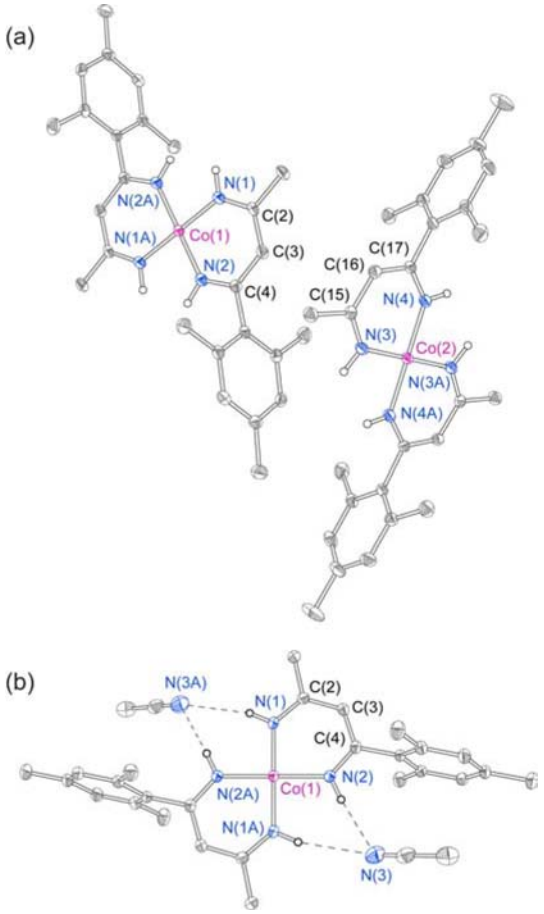

Figure 1. (a) X-ray crystal structure of the two independent molecules in **1** with 50% probability ellipsoids. Hydrogen atoms, excepting N−H, were omitted for clarity. Selected bond distances are reported in Table 1. Selected bond angles: N1−Co1−N2 = 90.00(5)°, N1−Co1−N2A = 90.00(5)°, N3−Co2−N4 = 90.15(5)°, N3−Co2−N4A = 89.85(5)°. (b) X-ray crystal structure of **1a** with 50% probability ellipsoids. Hydrogen atoms, excepting for N−H, were omitted for clarity. Selected bond distances are reported in Table 1. Selected bond angles: N1−Co−N2 = 90.60(5)°, N1−Co−N1A = 89.40(5)°.

structures show a square planar cobalt center ligated by two β-diketiminate ligands, with average Co−N bond distances of 1.87 and 1.86 Å, respectively (see Table 1). Compound **1** crystallizes in a solvent-free lattice with 2 independent molecules in the asymmetric unit. Each molecule lies on an inversion center in a fashion reminiscent of the structure of $(Me_6acac)_2Ni$.[38] Each molecule also displays a coplanar geometry of the core unit (nonmesityl) with nearly identical ∠N−Co−N bond angles of 90.0°, all of which sum to 360.0°.

In the case of **1a**, two molecules of acetonitrile are present, which show hydrogen bonding to the N−H functionalities, rather than coordination to the cobalt center. This hydrogen bonding induces a slight interligand ∠N−Co−N bond angle contraction to 89.4°, which is compensated by an intraligand bond angle expansion to 90.6°, retaining a planar CoN_4 molecular core.

Table 1. Crystallographic Bond Lengths (Å)

	1 Co1	1 Co2	1a	2
Co1−N1	1.864(1)		1.868(1)	1.870(2)
Co1−N2	1.854(1)		1.859(1)	1.868(2)
Co1−N3[a]		1.867(1)		1.871(2)
Co1−N4[a]		1.857(1)		1.872(2)
N1−C2	1.329(2)		1.330(2)	1.324(2)
N2−C4	1.333(2)		1.332(2)	1.328(2)
N3−C15		1.326(2)		1.325(2)
N4−C17		1.333(2)		1.328(2)
C2−C3	1.401(2)		1.399(2)	1.399(3)
C3−C4	1.396(2)		1.396(2)	1.397(3)
C15−C16		1.405(2)		1.397(3)
C16−C17		1.390(2)		1.393(3)

[a]For Co2 this corresponds to Co2−N3 and Co2−N4, respectively.

In benzene solution, complex **1** shows a room temperature magnetic moment of 2.4 μ_B as measured by Evans' method;[21] this magnetic moment compares closely to that of cobalt porphryin (2.42(5) μ_B).[39] Similar cobalt species are observed to distort to a pseudotetrahedral geometry accompanied by a spin crossover transition.[40−43] Compound **1** is not free to rotate in the crystalline state, and thus, the complex is locked into a square planar geometry and a low-spin ($S = {}^1/_2$) electronic configuration. In solution, however, the NacNac ligands may freely rotate with respect to each other, allowing the high spin isomer to contribute to the magnetic moment. DFT calculations suggest that the pseudotetrahedral high-spin ($S = {}^3/_2$) species is less than 1 kcal/mol higher in energy than the low-spin complex. Relaxed scans along the N−N−N−N dihedral angle of both high-spin and low-spin configurations gives a rotation barrier of 6 kcal/mol for the two spin-energy surfaces (Figure 2). The average Co−N bond length is 0.033 Å

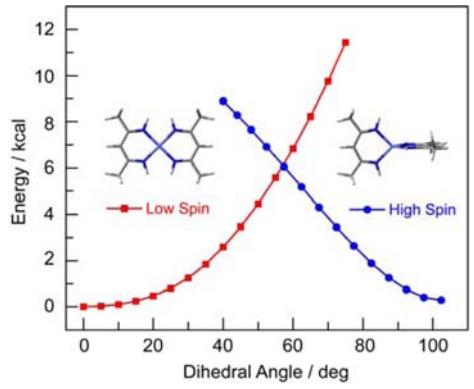

Figure 2. Relaxed potential energy surface scan of the N5−N2−N3−N4 dihedral angle of **1** in both low-spin ($S = {}^1/_2$) and high-spin ($S = {}^3/_2$) configurations. The intersection of these indicates that crossover occurs at a dihedral angle of approximately 57° with a 6 kcal/mol energy barrier.

longer in the calculated (1.892 Å) versus experimental (1.859 Å) structure of **1**, so the low-spin isomer might be more stable than the calculations suggest.

Figure 3 displays the EPR spectrum of **1**. A broad signal at g = 2.0 at room temperature splits to a rhombohedral signal at 77 K (toluene glass). The observed g-values of g_1 = 2.808, g_2 = 2.002, and g_3 = 1.956 are typical of related low spin planar Co(II) acacen,[44] salen,[45] and amben[46,47] complexes. The g_1

dx.doi.org/10.1021/ic301970w | Inorg. Chem. 2012, 51, 11190−11197

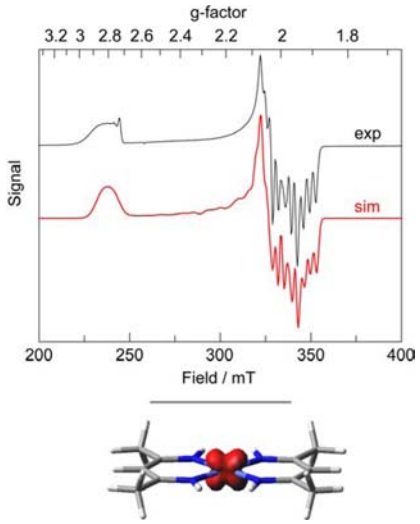

Figure 3. (Top) EPR of **1** in toluene glass at 77 K. Simulation yields *g*-values of g_1 = 2.808, g_2 = 2.002, and g_3 = 1.956 and *A*-values of A_x = 60.00 MHz, A_y = 74.03 MHz, and A_z = 97.23 MHz. (Bottom) Spin density plot of **1** showing unpaired electron localized on the metal based d_{yz} orbital (99%), isovalue 0.008.

value indicates a lack of apical coordination and significant electron delocalization along one axis. The g_3 value less than 2 corresponds to complexes characterized as having an unpaired electron in a d_{yz} orbital rather than a d_{z^2} orbital, which is commonly found in Co(II) oxime and porphyrin complexes.[48] Hitchman's equations correlating *g*-values with the electronic structure of Co(II) complexes gives roughly a 2300 cm^{-1} energy gap between the ground state $^2B_2(d_{yz})^1$ and the first excited state $^2A_1(d_{z^2})^1$.[49] DFT calculations establish that the SOMO of **1** is indeed of π-type b_2 symmetry, and the spin density is exclusively metal based (>99%, Figure 3, bottom).

The electronic absorption spectrum of **1** shown in Figure 4 is characterized by four pronounced UV transitions, which TD-

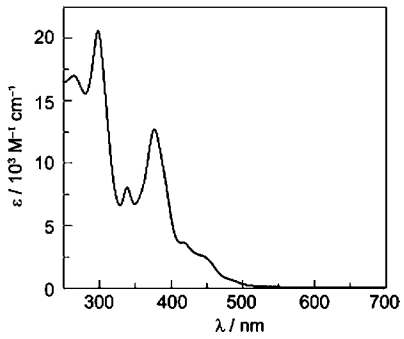

Figure 4. UV–vis spectrum of **1** in pentane.

DFT calculations suggest correspond to $\pi \rightarrow \pi^*$ and charge transfer transitions in the bis-NacNac ligand system (Figure S4). The π-system of **1** can be considered a subset of a porphyrin (Chart 1).

In this regard, it is not surprising to find that these transitions arise from transitions that are similar to the Soret and Q-bands of porphyrins, both in energy and intensity. The descent in symmetry from D_{4h} to C_{2v}, however, splits the degenerate e_g LUMO of a porphyrin into b_1 and b_2 type orbitals in complex **1**, giving rise to the additional transitions.

Chart 1

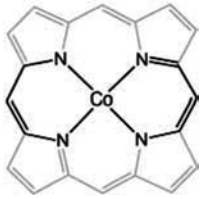

Figure 5 displays the cyclic voltammogram of **1**. One reversible oxidation event is observed within the solvent

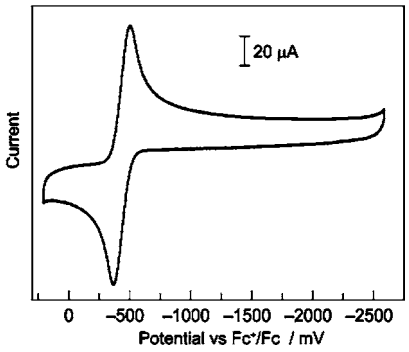

Figure 5. Cyclic voltammogram of **1** (1 mM) in THF with 0.1 M Bu_4NPF_6 supporting electrolyte at a scan rate of 100 mV/s and referenced vs ferrocene. Oxidation is centered at −434 mV.

windows of dichloromethane, acetonitrile, and THF. No reduction of **1** to a Co(I) species was observed. The oxidation potential of **1** in CH_2Cl_2 (Figure S6) is shifted 248 mV more positive than in THF. While differences in solvent dielectric and electrolyte ion pairing could shift the observed potential, this phenomenon is more likely due to the stabilization of **2** by THF coordination to the cobalt center. Alternatively, THF may be hydrogen bonding to the N–H protons of the ligand, stabilizing the planar isomer relative to the pseudotetrahedral one.

Characterization of 2. To characterize the oxidized species, **1** was treated with ferrocenium hexafluorophosphate in THF to yield complex **2**, which was isolated in 90% yield as a dark blue crystalline solid. Oxidation was also attempted in the absence of coordinating solvents, and although reaction in dichloromethane or benzene solutions proceeds similarly, a dark brown solid precipitated from the resulting dark blue solutions over the course of an hour. This decomposition was accelerated during attempts to crystallize the species as well as upon cooling. It was believed that the PF_6 counterion may react with the oxidized complex, though reaction of **1** with $FcBAr^F$ in noncoordinating solvents has also resulted in unstable dark blue solids.

The X-ray crystal structure of **2** (Figure 6) reveals a THF molecule bound apically to the cobalt center to give an approximate square-pyramidal geometry. Another THF molecule is hydrogen bound to two of the N–H in a fashion reminiscent of **1a**. Surprisingly, the Co–N bond distances have increased by 0.01 Å upon oxidation to 1.87 Å. This effect is perhaps due to weaker metal–ligand π interactions since the planes defining the NacNac ligands are each bent 5° away from the apical THF molecule. The structure also reveals that one of the NacNac ligands has rotated 180° with respect to the other to give a *cis* arrangement of the mesityl group.

dx.doi.org/10.1021/ic301970w | *Inorg. Chem.* 2012, 51, 11190–11197

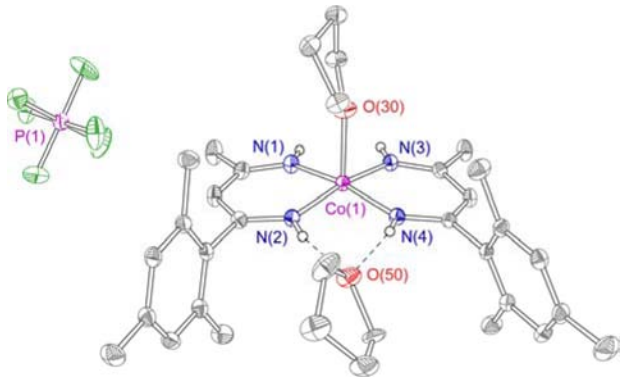

Figure 6. X-ray crystal structure of **2** with 50% probability ellipsoids. A THF molecule and hydrogen atoms, excepting N–H, were omitted for clarity. Selected bond distances are reported in Table 1. Selected bond angles: N1–Co–N2 = 90.29(7)°, N1–Co–N3 = 88.79(7)°, N2–Co–N4 = 88.94(7)°, N3–Co–N4 = 89.83(7)°, N1–Co–O30 = 94.88(6)°, N2–Co–O30 = 95.03(7)°, N3–Co–O30 = 96.03(7)°, N4–Co–O30 = 96.28(6)°.

A broad and intense band at 742 nm (Figure 7) gives rise to the observed blue color while a broad and weak absorption is

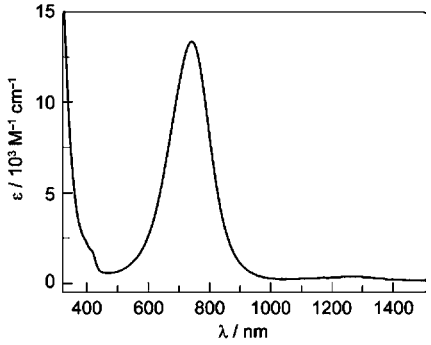

Figure 7. Absorption spectrum of **2** in THF.

observed at 1264 nm. Whereas these bands correspond to MLCT and IVCT transitions, respectively, in the tetrahedral Ni complexes, the molecular orbitals that give rise to the absorptions in **1a** are highly covalent in nature, and they possess significant metal and ligand character (Figure S5). Calculations and magnetic data (μ_{eff} = 3.21, by Evans' method) suggest that this paramagnetic species is a ground state triplet, which corresponds to one unpaired electron in d_{z^2} and one in an orbital that is shared between a metal d_{xz} orbital and a NacNac ligand π orbital; this spin density plot is shown in Figure 8.

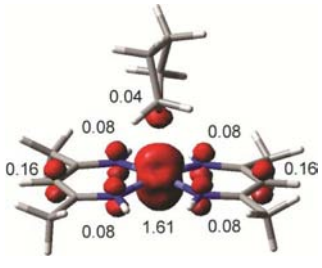

Figure 8. Spin density plot of **2** showing spin density both on the metal and ligand, isovalue = 0.008.

DISCUSSION

The insertion of acetonitrile to form **1** might imply that the Co(II)–mesityl bond is relatively polar to allow for nucleophilic attack on the nitrile functionality. This suggestion, however, would stand in contrast to the high covalency that is characteristic of late transition metal–aryl complexes. Moreover, a polar M–Ar bond would be strongly basic, and potentially favor deprotonation rather than insertion. Deprotonation of acetonitrile (pK_a (DMSO) = 31.3[50]) induces oligomerization reactions, and has been shown to produce isolable NacNac metal species derived from trimerization (eq 2).[51−56]

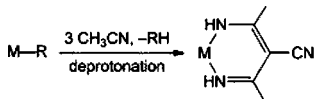

(2)

Although the fate of the extra equivalent of LiMes has not been determined in the synthesis of **1** from $Li(THF)_4CoMes_3$, it is reasonable to expect that it may indeed deprotonate and oligomerize acetonitrile, which is later removed from the reaction by filtration. The retention of two mesityl groups in **1** and the high isolated yields from both mesityl precursors strongly suggest that nitrile insertion is the dominant pathway (eq 3).

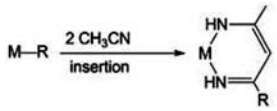

(3)

Acetonitrile insertion into a late metal–aryl bond has only been observed in a few circumstances: insertion into a palladium *ortho*-phenol species[57] and insertion into a Ni–mesityl bond to form a nickel–imine species.[58] In both cases, thallium salts of weakly coordinating anions induce abstraction of a coordinated halide and promote the binding of acetonitrile to the cationic metal complex. In contrast, the inherent coordinative unsaturation of Co_2Mes_4 likely induces binding of acetonitrile to form $(MeCN)_2CoMes_2$, which can then undergo metal-mediated insertion and condensation processes.

Nitrile insertion into late transition metals is rarely observed, especially in light of the functional tolerance of nitriles in cross-coupling and acrylonitrile polymerization reactions. On the basis of the few known examples,[52,53] it appears that nitrile insertion into late metal–carbon bonds has two critical requirements: a cationic or electron deficient metal center, and an open coordination site in a position *cis* to the alkyl or aryl moiety. Adhering to these criteria, acetonitrile insertion into metal alkyl or aryl species may provide a convenient route to unsubstituted NacNac complexes.

Although a planar structure has been suggested in related cobalt bis-NacNac complexes,[59−61] it is intriguing that no solvent molecules appear to bind to the apical positions of the metal. Indeed, there is no change in the absorption spectrum in pentane, THF, and acetonitrile solvents. The absence of axial ligands can be rationalized by the electronic structure of **1**. Scheme 2 outlines a qualitative molecular orbital diagram of **1** by mixing a σ-only d-orbital splitting diagram for a square planar d^7 metal complex (left) with the frontier π orbitals of the NacNac framework (right). The axes system utilized places the *z*-axis orthogonal to the plane of the bis-NacNac ligands and the *x*-axis and *y*-axis 45° rotated from the Co–N bonds. The π

dx.doi.org/10.1021/ic301970w | *Inorg. Chem.* 2012, 51, 11190−11197

Scheme 2

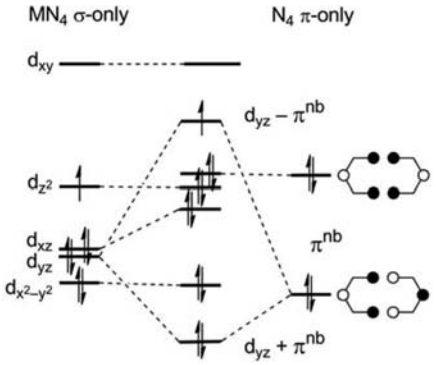

nonbonding orbital (with respect to the ligand) interacts with a d_{yz} orbital of the metal to transform the SOMO from a $^2A_1(d_{z^2})^1$ type orbital (left) to a delocalized orbital of $^2B_2(d_{yz})^1$ symmetry (center). Thus, the d_{z^2} orbital is filled in **1**, and the cobalt center gives expected planar geometry. That the SOMO is higher in energy than d_{z^2} is consistent with resistance of the metal complex to electrochemical reduction to a Co(I) species. Orbital population analysis from DFT calculations indicates that the $3d_{yz}$ orbital of Co is in fact only half occupied, as is indicated pictorially by the spin density plot of **1** (Figure 3).

The changes in electronic structure upon oxidation of **1** are governed by the binding of THF in **2**. Apical coordination of THF in **2** causes a corresponding rise in energy of the d_{z^2} orbital. Thus, **2** can be described as possessing a triplet ground state with d_{z^2} and d_{yz} SOMOs. The 3d orbitals are expected to become increasingly electronegative upon oxidation of the complex, resulting in a smaller energy difference between the metal and ligand orbitals. This causes an increase in ligand character of the d_{yz}-like SOMO. As a result, the spin density of **2** no longer resides solely on the metal, but also on the ligand (Figure 8). The spin density value of 1.61 on Co indicates that while the d_{z^2} type SOMO is mostly metal-centered, the d_{yz} SOMO is roughly 60% metal based and 40% ligand based. Although the oxidation state formalisms break down when considering redox-active ligands, the Co center in **2** could be best described as having an oxidation state of ca. 2.5.

The bond lengths of **1**, **1a**, and **2** are presented in Table 1. The Co−N bond lengths increase by an average of only 0.010(2) Å along the series. The C−N bond lengths of the ligand decrease by an average of 0.004(2) Å, a feature predicted by previous DFT calculations.[18] The C−C bond lengths do not change within error upon oxidation. The lack of significant Co−N bond length changes along with the paramagnetic nature of **2** gives clear evidence that the cobalt center does not experience a formal change in oxidation state upon oxidation of **1** to **2**. As predicted by simple molecular orbital theory, the oxidation of a NacNac ligand displays no significant structural change. Further support for oxidation of the NacNac ligand framework is provided by the intense visible absorption and calculated spin density.

Undoubtedly, one feature of **2** that allows isolation of a partially oxidized NacNac species is the presence of not one, but two coplanar NacNac ligands. If the radical was delocalized on only one ligand, structural changes may be unobserved owing to disorder in the crystal structure. The presence of a low energy absorption in the NIR suggests that this is not the case. Electronic communication between the ligands is conveyed through the d_{yz} orbital of the metal center, so that the molecule conveys class III delocalized radical cation.[62] Such behavior has been observed in an electronically related (salen)Ni^+ species.[63]

CONCLUSIONS

Because NacNac does not change structure upon oxidation, the presence of partially oxidized NacNac moieties can only be discerned with spectroscopy and computation. On the basis of the results described herein, and considering the ubiquitous presence of NacNac complexes in the literature, there is a possibility that the nature of some metal NacNac species have previously been misidentified. In these cases one would expect a metal in an oxidation state one level higher than the structure and reactivity warranted. While it is difficult to suggest redox behavior in these species without supporting calculations, some recently reported species[64,65] may warrant further investigation based on the results reported herein.

As indicated in Scheme 3, salen complexes have a similar π-type core, and indeed, redox noninnocence has been observed

Scheme 3

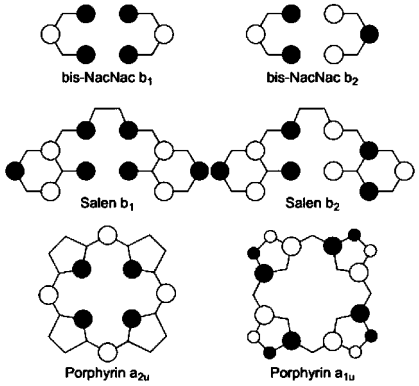

in some nickel species.[63,66−68] In these cases, the N_2O_2 coordination environment of the salen lowers the symmetry of noninnocent π orbital so that small but observable bond length changes do occur upon oxidation. On the other hand, cobalt salen complexes tend to axially coordinate additional ligands, raising the d_{z^2} orbital above d_{yz}. This axial coordination and the more electropositive nature of earlier first row transition metals likely stifle significant salen based redox-activity in other species.

Depending on the presence of certain *meso* substituents, the porphyrin HOMO could be either of a_{1u} or a_{2u} symmetry. While the a_{1u} orbital would generate observable bond length changes if oxidized, the a_{2u} orbital, which is related to the b_2 HOMO (middle-right, Scheme 3) of the bis-NacNac ligand framework of **1** and **2**, would not. In fact, complexes featuring porphyrin radical cations often show few structural changes relative to the neutral systems, though there often exists a strong tendency for intermolecular interactions in the solid state.[69] Nevertheless, these systems are likely another class of molecules that possess "hidden noninnocence".

Finally, acac complexes might be expected to behave similarly from an electronic standpoint, but the π nonbonding orbital is much less covalent, and consequently the ligand should be more difficult to oxidize. Cotton's unimolecular $(^tBu_2acac)_2Ni$ species[33] is perhaps an exemplar where oxidation could produce an acac radical species. Although this may prove too reactive to characterize structurally, acac complexes with significant spin density on the ligand do exist.[70]

dx.doi.org/10.1021/ic301970w | *Inorg. Chem.* 2012, 51, 11190−11197

Compound **1** represents a case where the ground state of the low-spin Co(II) molecule is $^2B_2(d_{yz})^1$ rather than $^2A_1(d_{z^2})$due to π donation from the ligands. The energy ordering of these two states strongly dictates the coordination and reactivity of the molecule. In the absence of a $^2A_1(d_{z^2})$ SOMO, **1** does not bind ligands axially, and this feature likely circumvents its reactivity with oxygen and electrochemical reduction to Co(I). Given the importance of planar cobalt species for mediating radical polymerization,[71] electrocatalytic hydrogen production,[72,73] and reversible oxygen transport,[74,75] understanding the nature ($^2B_2(d_{yz})^1$ vs $^2A_1(d_{z^2})$) of the ground state in each system is paramount for future ligand design and improvement of these catalytic reactions.

■ ASSOCIATED CONTENT

Ⓢ Supporting Information

Figures featuring additional characterization of **1** and **2**, Cartesian coordinates of the calculated species, and X-ray structure information (.cif). This material is available free of charge via the Internet at http://pubs.acs.org.

■ AUTHOR INFORMATION

Corresponding Author

*E-mail: nocera@mit.edu.

Notes

The authors declare no competing financial interest.

■ ACKNOWLEDGMENTS

We thank Dr. S. A. Stoian (CMU) for simulation of EPR data. This research was supported by the NSF CHE-1112154. Grants from the NSF also provided support to the DCIF at MIT (CHE-9808061 and DBI-9829592).

■ REFERENCES

(1) Chang, C. J.; Chng, L. L.; Nocera, D. G. *J. Am. Chem. Soc.* **2003**, *125*, 1866.
(2) McGuire, R., Jr.; Dogutan, D. K.; Teets, T. S.; Suntivich, J.; Shao-Horn, Y.; Nocera, D. G. *Chem. Sci* **2010**, *1*, 411.
(3) Soper, J. D.; Kryatov, S. V.; Rybak-Akimova, E. V.; Nocera, D. G. *J. Am. Chem. Soc.* **2007**, *129*, 5069.
(4) Dogutan, D. K.; McGuire, R., Jr.; Nocera, D. G. *J. Am. Chem. Soc.* **2011**, *133*, 9178.
(5) Dogutan, D. K.; Stoian, S. A.; McGuire, R., Jr.; Schwalbe, M.; Teets, T. S.; Nocera, D. G. *J. Am. Chem. Soc.* **2011**, *133*, 131.
(6) Schwalbe, M.; Dogutan, D. K.; Stoian, S. A.; Teets, T. S.; Nocera, D. G. *Inorg. Chem.* **2011**, *50*, 1368.
(7) Bachmann, J.; Hodgkiss, J. M.; Young, E. R.; Nocera, D. G. *Inorg. Chem.* **2007**, *46*, 607.
(8) Bachmann, J.; Nocera, D. G. *J. Am. Chem. Soc.* **2004**, *126*, 2829.
(9) Bachmann, J.; Nocera, D. G. *Inorg. Chem.* **2005**, *44*, 6930.
(10) Bachmann, J.; Nocera, D. G. *J. Am. Chem. Soc.* **2005**, *127*, 4730.
(11) Radosevich, A. T.; Melnick, J. G.; Stoian, S. A.; Bacciu, D.; Chen, C.-H.; Foxman, B. M.; Ozerov, O. V.; Nocera, D. G. *Inorg. Chem.* **2009**, *48*, 9214.
(12) Dempsey, J. L.; Esswein, A. J.; Manke, D. R.; Rosenthal, J.; Soper, J. D.; Nocera, D. G. *Inorg. Chem.* **2005**, *44*, 6879.
(13) Nocera, D. G. *Inorg. Chem.* **2009**, *48*, 10001.
(14) Kaim, W. *Inorg. Chem.* **2011**, *50*, 9752.
(15) Chirik, P. J. *Inorg. Chem.* **2011**, *50*, 9737.
(16) Haneline, M. R.; Heyduk, A. F. *J. Am. Chem. Soc.* **2006**, *128*, 8410.
(17) LeBlanc, F. A.; Berkefeld, A.; Piers, W. E.; Parvez, M. *Organometallics* **2012**, *31*, 810.
(18) Smith, A. L.; Hardcastle, K. I.; Soper, J. D. *J. Am. Chem. Soc.* **2010**, *132*, 14358.
(19) Kraft, S. J.; Williams, U. J.; Daly, S. R.; Kozimer, S. A.; Boland, K. S.; Kikkawa, J. M.; Forrest, W. P.; Christensen, C. N.; Schwarz, D. E.; Fanwick, P. E.; Clark, D. L.; Conradson, S. D.; Bart, S. C. *Inorg. Chem.* **2011**, *50*, 9838.
(20) Scarborough, C. C.; Sproules, S.; Weyhermueller, T.; DeBeer, S.; Wieghardt, K. *Inorg. Chem.* **2011**, *50*, 12446.
(21) Bourget-Merle, L.; Lappert, M. F.; Severn, J. R. *Chem. Rev.* **2002**, *102*, 3031.
(22) Mindiola, D. J. *Angew. Chem., Int. Ed.* **2009**, *48*, 6198.
(23) Khusniyarov, M. M.; Bill, E.; Weyhermuller, T.; Bothe, E.; Wieghardt, K. *Angew. Chem., Int. Ed.* **2011**, *50*, 1652.
(24) Theopold, K. H.; Silvestre, J.; Byrne, E. K.; Richeson, D. S. *Organometallics* **1989**, *8*, 2001.
(25) Le, B. J.; Jiao, H.; Meyer, W. E.; Hampel, F.; Gladysz, J. A. *J. Organomet. Chem.* **2000**, *616*, 54.
(26) Evans, D. F. *J. Chem. Soc.* **1959**, 2003.
(27) Becke, A. D. *Phys. Rev. A* **1988**, *38*, 3098.
(28) Becke, A. D. *J. Chem. Phys.* **1993**, *98*, 5648.
(29) Becke, A. D. *J. Chem. Phys.* **1993**, *98*, 1372.
(30) Lee, C. T.; Yang, W. T.; Parr, R. G. *Phys. Rev. B* **1988**, *37*, 785.
(31) Frisch, M. J.; Trucks, G. W.; Schlegel, H. B.; Scuseria, G. E.; Robb, M. A.; Cheeseman, J. R.; Montgomery, J. A., Jr.; Vreven, T.; Kudin, K. N.; Burant, J. C.; Millam, J. M.; Iyengar, S. S.; Tomasi, J.; Barone, V.; Mennucci, B.; Cossi, M.; Scalmani, G.; Rega, N.; Petersson, G. A.; Nakatsuji, H.; Hada, M.; Ehara, M.; Toyota, K.; Fukuda, R.; Hasegawa, J.; Ishida, M.; Nakajima, T.; Honda, Y.; Kitao, O.; Nakai, H.; Klene, M.; Li, X.; Knox, J. E.; Hratchian, H. P.; Cross, J. B.; Bakken, V.; Adamo, C.; Jaramillo, J.; Gomperts, R.; Stratmann, R. E.; Yazyev, O.; Austin, A. J.;Cammi, R.; Pomelli, C.; Ochterski, J. W.; Ayala, P. Y.; Morokuma, K.; Voth, G. A.; Salvador, P.; Dannenberg, J. J.; Zakrzewski, V. G.; Dapprich, S.; Daniels, A. D.; Strain, M. C.; Farkas, O.; Malick, D. K.; Rabuck, A. D.; Raghavachari, K.; Foresman, J. B.; Ortiz, J. V.; Cui, Q.; Baboul, A. G.; Clifford, S.; Cioslowski, J.; Stefanov, B. B.; Liu, G.; Liashenko, A.; Piskorz, P.; Komaromi, I.; Martin, R. L.; Fox, D. J.; Keith, T.; Al-Laham, M. A.; Peng, C. Y.; Nanayakkara, A.; Challacombe, M.; Gill, P. M. W.; Johnson, B.; Chen, W.; Wong, M. W.; Gonzalez, C.; Pople, J. A. *Gaussian 03*; Gaussian: Pittsburgh, PA, 2003.
(32) Schafer, A.; Huber, C.; Ahlrichs, R. *J. Chem. Phys.* **1994**, *100*, 5829.
(33) Schafer, A.; Horn, H.; Ahlrichs, R. *J. Chem. Phys.* **1992**, *97*, 2571.
(34) Bercaw, J. E.; Davies, D. L.; Wolczanski, P. T. *Organometallics* **1986**, *5*, 443.
(35) Barroso, S.; Cui, J.; Carretas, J. M.; Cruz, A.; Santos, I. C.; Duarte, M. T.; Telo, J. P.; Marques, N.; Martins, A. M. *Organometallics* **2009**, *28*, 3449.
(36) Richeson, D. S.; Mitchell, J. F.; Theopold, K. H. *J. Am. Chem. Soc.* **1987**, *109*, 5868.
(37) Richeson, D. S.; Mitchell, J. F.; Theopold, K. H. *Organometallics* **1989**, *8*, 2570.
(38) Cotton, F. A.; Wise, J. J. *Inorg. Chem.* **1966**, *5*, 1200.
(39) Dugad, L. B.; Marathe, V. R.; Mitra, S. *Chem. Phys. Lett.* **1985**, *120*, 239.
(40) Everett, G. W.; Holm, R. H. *J. Am. Chem. Soc.* **1965**, *87*, 5266.
(41) Everett, G. W.; Holm, R. H. *J. Am. Chem. Soc.* **1966**, *88*, 2442.
(42) Everett, G. W.; Holm, R. H. *Inorg. Chem.* **1968**, *7*, 776.
(43) Wolny, J. A.; Rudolf, M. F.; Ciunik, Z.; Gatner, K.; Wolowiec, S. *J. Chem. Soc., Dalton Trans.* **1993**, 1611.
(44) Hoffman, B. M.; Basolo, F.; Diemente, D. L. *J. Am. Chem. Soc.* **1973**, *95*, 6497.
(45) Busetto, C.; Cariati, F.; Fusi, A.; Gullotti, M.; Morazzon., F; Pasini, A.; Ugo, R.; Valenti, V. *J. Chem. Soc., Dalton Trans.* **1973**, 754.
(46) Malatesta, V.; McGarvey, B. R. *Can. J. Chem.* **1975**, *53*, 3791.
(47) Urbach, F. L.; Bereman, R. D.; Topich, J. A.; Harihara., M.; Kalbache, B. *J. Am. Chem. Soc.* **1974**, *96*, 5063.
(48) La Mar, G. N.; Walker, F. A. *J. Am. Chem. Soc.* **1973**, *95*, 1790.
(49) Hitchman, M. A. *Inorg. Chem.* **1977**, *16*, 1985.

(50) Matthews, W. S.; Bares, J. E.; Bartmess, J. E.; Bordwell, F. G.; Cornforth, F. J.; Drucker, G. E.; Margolin, Z.; McCallum, R. J.; McCollum, G. J.; Vanier, N. R. *J. Am. Chem. Soc.* **1975**, *97*, 7006.
(51) Michelin, R. A.; Mozzon, M.; Bertani, R. *Coord. Chem. Rev.* **1996**, *147*, 299.
(52) Antunes, M. A.; Dias, M.; Monteiro, B.; Domingos, A.; Santos, I. C.; Marques, N. *Dalton Trans.* **2006**, 3368.
(53) Kopp, M. R.; Neumüller, B. *Z. Anorg. Allg. Chem.* **1999**, *625*, 1246.
(54) Nishijo, J.; Nishi, N. *Eur. J. Inorg. Chem.* **2006**, *15*, 3022.
(55) Redshaw, C.; Jana, S.; Shang, C.; Elsegood, M. R. J.; Lu, X.; Guo, Z. X. *Chem. Commun.* **2010**, 46.
(56) Yuan, J.; Hughes, R. P.; Rheingold, A. L. *Organometallics* **2009**, *28*, 4646.
(57) Vicente, J.; Bad, J. A.; Lopez-Saez, M. J.; Jones, P. G. *Angew. Chem., Int. Ed.* **2005**, *44*, 6001.
(58) Ceder, R. M.; Muller, G.; Ordinas, M.; Ordinas, J. I. *Dalton Trans.* **2007**, 83.
(59) Hitchcock, P. B.; Lappert, M. F.; Linnolahti, M.; Sablong, R.; Severn, J. R. *J. Organomet. Chem.* **2009**, *694*, 667.
(60) Hitchcock, P. B.; Lappert, M. F.; Liu, D. S. *J. Chem. Soc., Chem. Commun.* **1994**, 1699.
(61) McGeachin, S. G. *Can. J. Chem.* **1968**, *46*, 1903.
(62) Robin, M. B.; Day, P. *Adv. Inorg. Chem. Radiochem.* **1967**, *10*, 247.
(63) Storr, T.; Wasinger, E. C.; Pratt, R. C.; Stack, T. D. P. *Angew. Chem., Int. Ed.* **2007**, *46*, 5198.
(64) Conradie, J.; Ghosh, A. *J. Chem. Theory Comput.* **2007**, *3*, 689.
(65) Shaffer, D. W.; Ryken, S. A.; Zarkesh, R. A.; Heyduk, A. F. *Inorg. Chem.* **2011**, *50*, 13.
(66) Shimazaki, Y.; Yajima, T.; Tani, F.; Karasawa, S.; Fukui, K.; Naruta, Y.; Yamauchi, O. *J. Am. Chem. Soc.* **2007**, *129*, 2559.
(67) Shimazaki, Y.; Stack, T. D. P.; Storr, T. *Inorg. Chem.* **2009**, *48*, 8383.
(68) Kurahashi, T.; Fujii, H. *J. Am. Chem. Soc.* **2011**, *133*, 8307.
(69) Kadish, K. M.; Smith, K. M.; Guilard, R. *The Porphyrin Handbook*; Academic Press: San Diego, CA; Vol. *3*, 1999.
(70) Das, A.; Scherer, T. M.; Chowdhury, A. D.; Mobin, S. M.; Kaim, W.; Lahiri, G. K. *Inorg. Chem.* **2012**, *51*, 1675.
(71) Debuigne, A.; Poli, R.; Jerome, C.; Jerome, R.; Detrembleur, C. *Prog. Polym. Sci.* **2009**, *34*, 211.
(72) Artero, V.; Chavarot-Kerlidou, M.; Fontecave, M. *Angew. Chem., Int. Ed.* **2011**, *50*, 7238.
(73) Dempsey, J. L.; Brunschwig, B. S.; Winkler, J. R.; Gray, H. B. *Acc. Chem. Res.* **2009**, *42*, 1995.
(74) Crumblis, A.; Basolo, F. *Science* **1969**, *164*, 1168.
(75) Tine, M. R. *Coord. Chem. Rev.* **2012**, *256*, 316.